

MIT Open Access Articles

*Controlling the Fibroblastic Differentiation of
Mesenchymal Stem Cells Via the Combination of
Fibrous Scaffolds and Connective Tissue Growth Factor*

The MIT Faculty has made this article openly available. **Please share**
how this access benefits you. Your story matters.

Citation: Tong, Zhixiang et al. "Controlling the Fibroblastic Differentiation of Mesenchymal Stem Cells Via the Combination of Fibrous Scaffolds and Connective Tissue Growth Factor." *Tissue Engineering Part A* 17.21-22 (2011): 2773-2785. Web. 20 Jan. 2012. © 2011 Mary Ann Liebert, Inc.

As Published: <http://dx.doi.org/10.1089/ten.tea.2011.0219>

Publisher: Mary Ann Liebert, Inc.

Persistent URL: <http://hdl.handle.net/1721.1/68627>

Version: Final published version: final published article, as it appeared in a journal, conference proceedings, or other formally published context

Terms of Use: Article is made available in accordance with the publisher's policy and may be subject to US copyright law. Please refer to the publisher's site for terms of use.



Controlling the Fibroblastic Differentiation of Mesenchymal Stem Cells Via the Combination of Fibrous Scaffolds and Connective Tissue Growth Factor

Zhixiang Tong, B.S.,¹ Shilpa Sant, Ph.D.,²⁻⁴ Ali Khademhosseini, Ph.D.,²⁻⁴ and Xinqiao Jia, Ph.D.^{1,5}

Controlled differentiation of multi-potent mesenchymal stem cells (MSCs) into vocal fold-specific, fibroblast-like cells *in vitro* is an attractive strategy for vocal fold repair and regeneration. The goal of the current study was to define experimental parameters that can be used to control the initial fibroblastic differentiation of MSCs *in vitro*. To this end, connective tissue growth factor (CTGF) and micro-structured, fibrous scaffolds based on poly(glycerol sebacate) (PGS) and poly(ϵ -caprolactone) (PCL) were used to create a three-dimensional, connective tissue-like microenvironment. MSCs readily attached to and elongated along the microfibers, adopting a spindle-shaped morphology during the initial 3 days of preculture in an MSC maintenance medium. The cell-laden scaffolds were subsequently cultivated in a conditioned medium containing CTGF and ascorbic acids for up to 21 days. Cell morphology, proliferation, and differentiation were analyzed collectively by quantitative PCR analyses, and biochemical and immunocytochemical assays. F-actin staining showed that MSCs maintained their fibroblastic morphology during the 3 weeks of culture. The addition of CTGF to the constructs resulted in an enhanced cell proliferation, elevated expression of fibroblast-specific protein-1, and decreased expression of mesenchymal surface epitopes without markedly triggering chondrogenesis, osteogenesis, adipogenesis, or apoptosis. At the mRNA level, CTGF supplement resulted in a decreased expression of collagen I and tissue inhibitor of metalloproteinase 1, but an increased expression of decorin and hyaluronic acid synthetase 3. At the protein level, collagen I, collagen III, sulfated glycosaminoglycan, and elastin productivity was higher in the conditioned PGS-PCL culture than in the normal culture. These findings collectively demonstrate that the fibrous mesh, when combined with defined biochemical cues, is capable of fostering MSC fibroblastic differentiation *in vitro*.

Introduction

THE HUMAN VOCAL FOLDS, composed of a pliable lamina propria sandwiched between a stratified squamous epithelial layer and the vocalis muscle, are particularly adapted to sound production.¹ Under normal circumstances, vocal folds can sustain up to 30% strain at frequencies of 100 to 1000 Hz.² Numerous deleterious factors can lead to vocal fold damage and dysfunction,³ for which long-term, satisfactory treatments do not exist. The inability to articulate sounds renders vocal fold patients socially isolated. The development of tissue engineering strategies for the reconstruction of vocal folds will not only offer alternative treatment for vocal fold disorders but also provide an *in vitro* platform for the investigation of vocal fold diseases. Suc-

cessful engineering of vocal fold tissue relies on a strategic combination of viable cells, biomimetic matrices, biological factors, and biomechanical stimulations.

If one wishes to engineer a functional vocal fold lamina propria, theoretically, one has to take a healthy biopsy from the patient's vocal fold to isolate primary vocal fold fibroblasts for subsequent cell culture. Such an operation induces more damage to the already compromised vocal fold lamina propria. Even if these cells are successfully isolated, sufficient numbers of cells cannot be obtained. Under current *in vitro* conditions, human vocal fold fibroblasts possess a relatively short replicative life span. After a series of population doublings, primary cells enter a state in which they no longer divide, marked by distinct changes in cell morphology, gene expression, and metabolism.⁴ On the other hand, bone

¹Department of Materials Science and Engineering, Delaware Biotechnology Institute, University of Delaware, Newark, Delaware.

²Department of Medicine, Center for Biomedical Engineering, Harvard Medical School, Brigham and Women's Hospital, Cambridge, Massachusetts.

³Harvard-MIT Division of Health Sciences and Technology, Massachusetts Institute of Technology, Cambridge, Massachusetts.

⁴Wyss Institute for Biologically Inspired Engineering, Harvard University, Boston, Massachusetts.

⁵Department of Biological Sciences, University of Delaware, Newark, Delaware.

marrow-derived, mesenchymal stem cells (MSCs) can be readily aspirated as a clinically accepted procedure; they are capable of self-renewal, and have been widely explored as a therapeutic cell source for a variety of regenerative medicine applications.^{5,6} MSCs have been successfully differentiated into osteoblasts, chondrocytes, adipocytes, and nerve cells under defined culture conditions.⁶ The fibroblastic differentiation of MSCs, however, has been relatively unexplored due to the remarkable diversity of tissue origins, phenotypes, and lack of unique markers for fibroblast.⁷⁻⁹

It is well known that stem cell fate can be specified by the physical and chemical characteristics of their surrounding matrices, as well as various regulatory factors.¹⁰⁻¹³ Synthetic scaffolds that resemble the native extracellular matrix (ECM) morphologically and functionally are highly desirable for programmed MSC differentiation and vocal fold tissue engineering.¹⁴ Over the past decade, electrospinning¹⁵ has emerged as a highly promising process for producing tissue engineering constructs since the resulting scaffolds possess many of the desired properties, such as a high surface-to-volume ratio, high porosity, and an interconnected three-dimensional (3D) porous network.^{16,17} Various natural or synthetic materials have been electrospun into fibrous scaffolds with desirable morphology and tissue-like mechanical properties.¹⁸ A new type of biocompatible and biodegradable polyester elastomer based on poly(glycerol sebacate) (PGS) has garnered considerable attention recently.¹⁹⁻²³ PGS prepolymer can be easily processed into porous scaffolds via electrospinning, photo-crosslinking, or simply blending with other carrier material, such as poly(ϵ -caprolactone) (PCL). These scaffolds have been shown to regulate cell attachment, proliferation, and orientation.^{19,20,24,25} Compared to the PCL counterpart, fibrous scaffolds fabricated from a physical blend of PGS and PCL are softer and more pliable, having an ultimate elongation of 400%–500%.¹⁹ Such elastomeric scaffolds may provide the necessary mechanical environment for highly dynamic tissues such as vocal folds.

Soluble biological factors are potent regulators of cell fate. Connective tissue growth factor (CTGF) is a 36–38 kDa heparin-binding multi-domain protein.²⁶ It is involved in a wide spectrum of physiological and pathological events, such as embryo development, angiogenesis, and wound healing.^{27,28} With respect to connective tissue function, CTGF has been shown to affect fibroblast proliferation, motility, adhesion, and ECM synthesis.²⁷ The biological activities of CTGF suggest its utility in controlled differentiation of MSCs into vocal fold fibroblasts. Mao and co-workers²⁹ recently reported that CTGF alone is sufficient to induce fibrogenesis *in vitro*. Particularly, CTGF-treated MSCs lost their surface mesenchymal epitopes and tri-lineage potential after fibroblastic commitment, expressed broad fibroblastic markers at gene and protein level, and maintained their potential to differentiate into myofibroblasts upon TGF- β 1 treatment.

The ultimate goal of our investigation is to promote the assembly of vocal fold-like ECM by MSC-derived fibroblast cells. In the current proof-of-concept investigation, we assess the ability of electrospun PGS-PCL scaffolds to support the attachment, proliferation, and fibroblastic differentiation of MSCs cultured in a CTGF-conditioned medium. We hypothesize that the PGS-PCL scaffold combined with exogenous biochemical cues can synergistically stimulate the fibroblastic differentiation of MSCs. Fibrous scaffolds with a

PGS:PCL weight ratio of 2:1 was chosen due to their consistent fiber morphology, elastomeric properties, and cell adhesive characteristics.¹⁹ MSCs were seeded on the scaffolds and were cultivated in the maintenance media with or without CTGF and ascorbic acid supplement. The advantages of the 3D fibrous scaffold were verified by a parallel comparison with cells cultured on tissue culture polystyrene (TCPS). Cell morphology, proliferation, gene expression, and ECM synthesis were evaluated systematically after 21 days of cultivation. The fibroblastic differentiation was verified by the upregulation of fibroblast-specific protein-1 (FSP-1), a fibroblast-specific protein,³⁰ and the diminished ability of MSCs to undergo chondrogenesis, adipogenesis, osteogenesis, and myogenesis.⁶ Modulated production of essential ECM proteins has also been observed.

Materials and Methods

Scaffold fabrication

PGS was synthesized by condensation polymerization of glycerol and sebacic acid, following a previously reported procedure.²⁴ PCL with a molecular weight of 70–90 kDa was purchased from Sigma Aldrich. PGS and PCL were dissolved in chloroform/ethanol (9:1, v/v) at a total polymer concentration of 33 wt% with a PGS: PCL weight ratio of 2:1. The polymer solution was spun at a flow rate of 2 mL/h for ~30 min with an applied voltage of 15 kV. Fibers were collected on the nonadhesive side of a tape attached to a copper wire frame that was wrapped about a glass slide, as described previously.¹⁹ The collected fibers were dried overnight under vacuum. The morphology of the PGS-PCL scaffold was characterized using a Field Emission Scanning Electron Microscope (Ultra 55; Carl Zeiss). Scaffolds (8.5×5 mm) were tightly secured on the bottom of a cell culture insert (Millipore), soaked in 70% ethanol overnight with gentle shaking, rinsed with Dulbecco's phosphate-buffered saline (DPBS; Invitrogen), and UV-sterilized for 15 min. Finally, scaffolds were equilibrated in the normal MSC maintenance medium containing 10% fetal bovine serum (Lonza) in a humidified incubator at 37°C for 2–3 h before cell seeding. Our sterilization protocol was developed to maximize the germicidal effects without compromising the scaffold integrity.

Cell culture

Human bone marrow-derived MSCs were purchased from Lonza. Cells were sub-cultured at a seeding density of 5000–6000 cells/cm² on T-150 flasks (Corning) at 37°C with 5% CO₂ in the normal media. Medium was refreshed every 3 days. Upon reaching ~80% confluence, cells were trypsinized, resuspended in the same medium, and subsequently added to the PGS-PCL scaffold at a density of 0.2 million cells per mesh. Cells were allowed to attach for 1.5–2 h before additional medium was introduced. The constructs were precultured in the normal media in a humidified incubator (37°C, 5% CO₂) without any disturbance for 3 days. The normal medium was subsequently replaced with the conditioned medium supplemented with 100 ng/mL CTGF (Biovendor) and 50 μ g/mL L-ascorbic acids (Sigma Aldrich). To simplify our discussion, the end of 3-day preculture is designated as day 0 of the subsequent conditioned culture. Medium was changed every day to ensure the biological activities of CTGF, and constructs

were collected at day 0, 7, 14, and 21 for the respective biochemical and immunocytochemical analyses. Control experiments were carried out in the absence of CTGF under the same conditions. Parallel experiments with MSCs cultured on TCPS (Nunc) were also performed.

Cell viability and morphology

At a predetermined time, the constructs were rinsed with DPBS, stained with propidium iodide (1:2000 in DPBS; Invitrogen) and Syto-13 (1:1000 in DPBS; Invitrogen) for 5 min, and imaged with a Zeiss LSM 510 Axiovert Confocal Microscope. Separately, a commercially available actin cytoskeleton and focal adhesion staining kit (Millipore) was utilized to assess cell morphology and attachment. Briefly, constructs were rinsed in DPBS, fixed in 4% paraformaldehyde (Electron Microscope Science) for 15 min, and permeabilized in 0.1% Triton X-100 (Fisher) on ice for 5 min. Constructs were subsequently blocked with 3% heat-inactivated bovine serum albumin (BSA; Jackson ImmunoResearch) in DPBS for 30 min, followed by a 1-h incubation in vinculin primary antibody (1:100 in 1% BSA; Millipore). Samples were subsequently costained with Alexa Fluor[®] 488 goat anti-mouse IgG (Invitrogen; 1:100 in 1% BSA) and TRITC-conjugated Phalloidin (Millipore; 1:200 in 1% BSA) for another hour. Finally, constructs were counterstained with drq-5 (1:1000 in DPBS; Axxora LLC) or DAPI (1:1000 in DPBS; Millipore) for 5 min before being imaged by Zeiss LSM 510 confocal microscope.

Cell proliferation

Constructs were collected at predetermined times, rinsed in a cold DPBS, snap-frozen in liquid nitrogen, lyophilized, and accurately weighed. Samples were subsequently digested in a 20 mM Na₂HPO₄ solution containing 300 µg/mL papain, 5 mM EDTA, and 2 mM dithiothreitol at a pH of ~6.5 and temperature of 65°C for 18 h (all digestion reagents were purchased from Sigma).³¹ The digestion mixtures were centrifuged at 13,000 rpm to remove the insoluble scaffold debris. The total dsDNA was quantified by picogreen DNA assay (Invitrogen) following an established protocol.³²

Briefly, 10 µL of the digested samples was diluted in a Tris-HCl/EDTA buffer to a final volume of 1.0 mL. One milliliter picogreen working solution was added to each sample and incubated for 2–5 min at room temperature in the dark. Using a PerkinElmer microplate reader, the solutions were excited at 485 nm and the intensity of the fluorescence emission was measured at 530 nm. The standard curve was prepared using dsDNA provided in the assay.

Gene expression

The snap-frozen constructs were crushed with a pestle and digested in a Trizol (Invitrogen)/chloroform (5/1 v/v) mixture. The digestion mixture phase separated into three layers: an aqueous RNA layer (top), a middle DNA layer, and a bottom organic layer containing total proteins.^{33,34} The RNA layer was carefully aspirated and stored at –80°C. RNA was retrieved from the aqueous phase by precipitation in isopropanol, followed by centrifugation (13,000 rpm, 10 min) and thorough washing (twice with 75% ethanol) before being reconstituted in RNase-free H₂O (Invitrogen). The RNA concentration was determined using a Nanodrop ND-1000 Spectrophotometer (Nanodrop Technologies). Each RNA sample (0.5 µg) was reverse transcribed into cDNA using a QuantiTect Reverse Transcription kit (Qiagen) following the manufacturer's procedure. Sequence-specific amplification from cDNA was performed and quantitatively detected by an ABI 7300 real-time PCR system using SYBR green PCR master mix (Applied Biosystems). PCR thermal cycle was programmed into three stages: initialization at 95°C for 10 min, denaturation at 95°C for 15 s, and annealing at 60°C for 1 min (total 45 cycles). The purity of the PCR product was confirmed by the dissociation curve, constructed by sequential heating of the product (95°C for 15 s, 60°C for 60 s, and 95°C for 15 s). Primer sequences for collagen type I (COL I), elastin (ELA), decorin (DEC), tissue inhibitor of metalloproteinases 1 (TIMP1), HA synthase 3 (HAS3), CD44, FSP-1, adipocyte fatty acid binding protein (aP2), alkaline phosphatase (ALP), aggrecan (AGG), and apoptosis indicator p53 are listed in Table 1. Glyceraldehyde-3-phosphate dehydrogenase (GAPDH) was used as the house keeping gene. All primers were synthesized by Integrated DNA technologies.

TABLE 1. SUMMARY OF QUANTITATIVE POLYMERASE CHAIN REACTION PRIMERS USED IN THIS STUDY

Gene	Forward primer (5'–3')	Reverse primer (5'–3')	GenBank no.	Product size (bp)
COL I ³⁹	AACAAATAAGCCATCACGCCT	TGAAACAGACTGGGCCAATGTC	NM_000089	101
ELA ⁶⁰	AAAGCAGCAGCAAAGTTCGG	ACCTGGGAC AACTGGAATCC	NM_001081755	274
DEC ⁶¹	GATGCAGCTAGC CTGAAAGG	TCACACCCGAATAAGAAGCC	NM_133503	274
TIMP1	TTTCTTGGTTCCCCAGAATG	CAGAGCTGCAGAGCAACAAG	NG_012533	99
HAS3 ⁶²	TGTGCAGTGTATTAGTGGGCCCTT	TTGGAGCGCGTATACTTAGTT	NM_005329	177
CD44 ⁶³	TGCCGCTTTGCAGGTGTAT	GGCCTCCGTCCGAGAGA	NM_001001392	70
FSP-1 ⁶⁴	AGCTTCTTGGGAAAAGGAC	CCCCAACCACAT CAGAGG	NM_019554	200
aP2 ⁶⁵	TCAGTGTGAATGGGGATGTG	GTGGAAGTGACGCCTTTCAT	NM_001442	250
ALP ⁶⁶	TGGAGCTTCAGAAGCTCAACACCA	ATCTCGTTGTCTGAGTACCAGTCC	NM_000478	454
AGG ⁶⁶	TCGAGGACAGCGAGGCC	TCGAGGGTGTAGCGTGTAGAGA	NM_013227	85
p53 ⁶⁷	TGCGTGTGGAGTATTTGGATG	GTGTGATGATGGTGAGGATGG	NM_000546	168
GAPDH ⁶⁸	GAAATCCCATCACCATCTTCCAGG	GAGCCCCAGCCTTCTCCATG	NM_002046	120

Primer sequences for TIMP1 was designed based on gene sequence obtained from GenBank (NG_012533) using Primer 3 software (<http://frodo.wi.mit.edu/primer3/>). All other primer sequences were based on published records and the respective GenBank numbers are included in the table.

The relative gene expression (fold change) was calculated with respect to *GAPDH* and was normalized against day 0 or the respective normal culture using $2^{\Delta\Delta C_t}$ method.^{35,36}

Immunocytochemical analysis

Constructs were fixed, permeabilized, and blocked following same procedure described above for actin/viculin staining. After blocking, samples were incubated overnight at 4°C with primary antibodies for collagen I and III (mouse-derived monoclonal antibodies from Abcam) at a dilution factor of 1:200 (in 1% BSA). Additionally, muscle-specific actin (MSA) and STRO-1 were stained by MSA Ab-4 and mouse anti-human STRO-1 antibody (1:50 dilution in 1% BSA; Invitrogen), respectively. Constructs stained for STRO-1 were fixed in a cold methanol for 20 min before blocking. Samples were subsequently counterstained with Alexa-488 goat anti-mouse IgG (1:200 dilution with 1% BSA) for 1 h in the dark and DAPI (1:1000 in DPBS) for 5 min before being imaged with an LSM 5 Live high-speed confocal microscope (Zeiss). Z-stacked Images were analyzed by Volocity 3D-4D imaging software (PerkinElmer) for semi-quantitative analysis of the protein expression. The fluorescence intensities for the protein and the cell nuclei were acquired by summarizing the total green and blue pixels through the total thickness of the membrane. Protein production was expressed either as the fluorescence intensity of the protein or divided by the number of the nuclei, both of which were normalized to the respective baseline levels at day 0.

Biochemical analysis

The production of sulfated glycosaminoglycan (sGAG) and insoluble elastin was quantified biochemically. For sGAG quantification, constructs were digested following the procedure described above for DNA quantification. The digestion aliquots (60 μ L) were mixed with the papain digestion buffer (40 μ L) and sGAG content was analyzed using a Blyscan sGAG Assay (Biocolor). The diluted samples, the standards, and the blank digestion buffer (100 μ L) were mixed with 1,9-dimethyl-methylene blue solution (1 mL) and were incubated at room temperature for 45 min. The resulting dye-sGAG complex was precipitated by centrifugation (14,000 rpm for 10 min), and the soluble unbound dye was aspirated. The dissociation reagent (700 μ L) was subsequently added to the complex to release the bound dye. The sample absorbance was recorded using a Beckman Coulter microplate reader at 620 nm. Fastin elastin assay kit (Biocolor) was employed for elastin analysis. Constructs were digested in Trizol/chloroform, as described above for gene analysis. After the RNA and the DNA layers were removed, cold acetone (Sigma) was added to precipitate proteins from the organic phase. The protein pellets collected were thoroughly washed with guanidine hydrochloride (0.3 M in ethanol; Sigma), followed by ethanol (with 2.5% glycerol) and vacuum dried for 5–10 min. Oxalic acid (0.2 mL 0.25 M in H₂O; Sigma) was added to each protein pellet and the mixture was boiled at 99°C for 1–2 h to completely solubilize the protein. The solubilized protein containing the elastin extract was precipitated overnight at 4°C by adding 1 mL Fastin precipitating reagent. The collected pellet (14,000 rpm for 10 min) was mixed with Fastin dye reagent for 90 min. The elastin dye was mixed with 200 μ L dissociation reagent (200 μ L) for 45 min under gentle agitation (1000 rpm) in the dark. Finally, the

absorbance of recovered dye, α -elastin standards, and blanks was recorded at 590 nm using a Beckman Coulter microplate reader.

Statistical analysis

All data were reported as the mean value \pm standard error of 3–7 repeats. Student's two-tailed *t*-test was employed to determine the significant differences between groups, with $p < 0.05$ being considered as statistically different.

Results

In this study, we assessed the ability of fibrous scaffolds derived from PGS and PCL to support the growth, attachment, and proliferation of MSCs. We further investigated whether the addition of CTGF in the culture media could foster the fibroblastic differentiation of MSCs. First, a short-term comparative experiment was conducted to understand the substrate-induced, differential responses of MSCs to CTGF treatment. Subsequently, MSCs were loaded in the fibrous scaffolds and cultured with or without CTGF for various times. Cellular behaviors were assessed using qPCR and standard immunocytochemical/biochemical analyses.

Effects of substrate on MSC response to CTGF

Using qPCR, we quantified the effects of CTGF supplement on MSC gene expression after 7 days of culture on two different substrates: traditional TCPS plates and fibrous PGS-PCL scaffolds. The relative expression of important ECM proteins (*COL I*, *ELA*, *DEC*, *HAS3*, and *TIMP1*), stem cell differentiation (*CD44*, *FSP-1*, *aP2*, *ALP*, and *AGG*), and apoptosis (*p53*) markers was analyzed. The specificity of the PCR primers (Table 1) was confirmed by melting curves (data not shown) and the gene expression was normalized to the respective normal cultures. In the case of TCPS culture, CTGF supplement significantly ($p < 0.05$) increased the expression

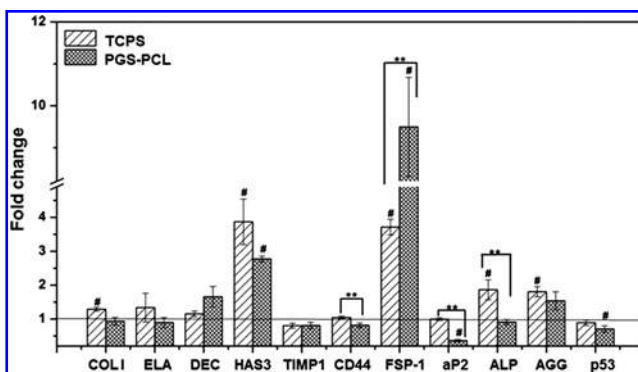


FIG. 1. Differential effects of CTGF on gene expression of MSCs cultured on TCPS plates or in PGS-PCL scaffolds. qPCR analysis was conducted after 7 days of culture. *GAPDH* was used as an internal control, and the gene expression was normalized to the respective CTGF-free culture. #Significant difference ($p < 0.05$) between the normal and the conditioned cultures; **significant difference ($p < 0.05$) between TCPS and PGS-PCL cultures. MSC, mesenchymal stem cell; CTGF, connective tissue growth factor; PGS, poly(glycerol sebacate); PCL, poly(ϵ -caprolactone); TCPS, tissue culture polystyrene; *GAPDH*, glyceraldehyde-3-phosphate dehydrogenase.

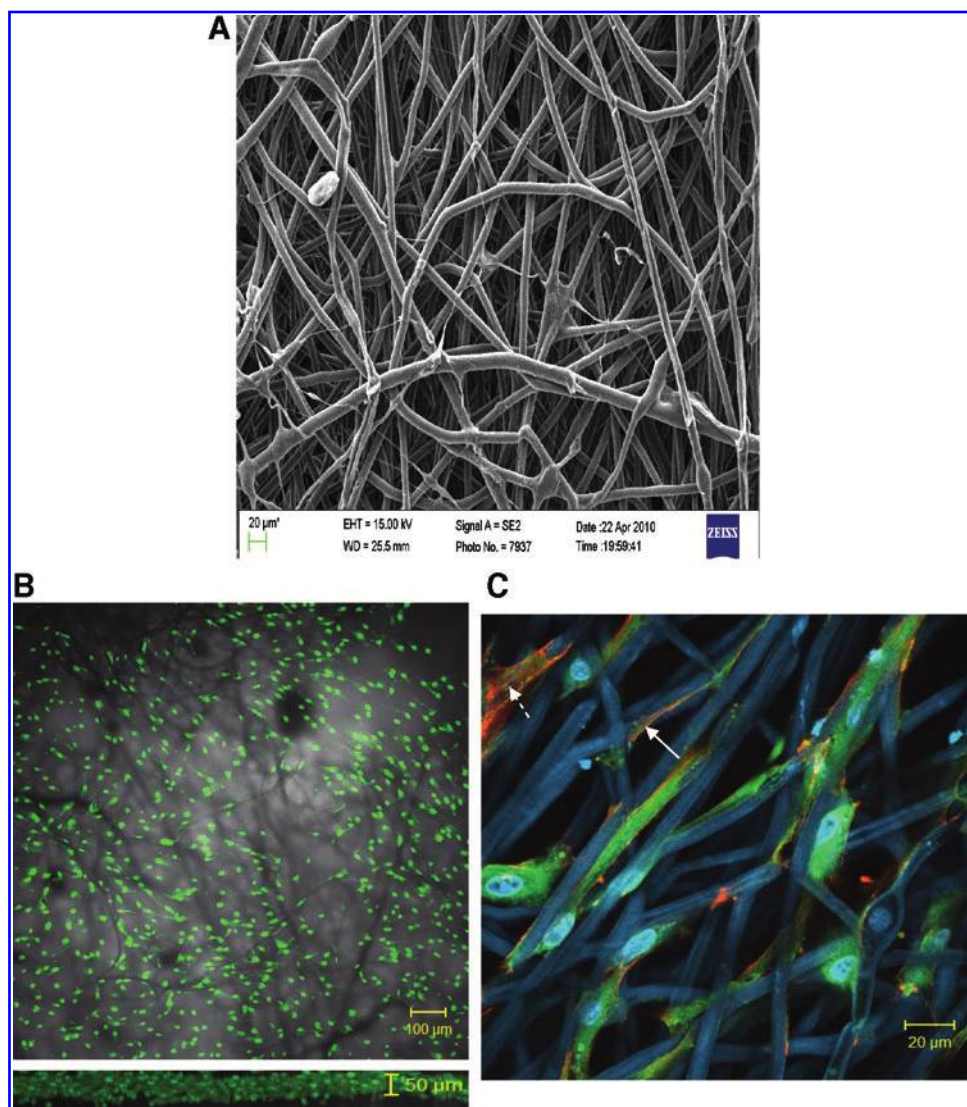


FIG. 2. Characterization of PGS-PCL scaffolds in terms of their microstructure (**A**) and their ability to support MSC culture (**B, C**). (**A**) Field emission scanning electron microscope micrograph of a PGS-PCL scaffold. (**B**) Representative live/dead staining of MSCs after 3 days of preculture in the normal media. Live cells (green) and dead cells (red) were stained by Syto 13 and propidium iodide, respectively. The top panel is a top view of the confocal image overlapped with the phase contrast image. The bottom panel shows the side view of the constructs with 50 μm sampling depth. (**C**) Representative F-actin/vinculin costaining of MSCs after 3 days of preculture in the normal media. F-actin filaments were stained red by TRITC-phalloidin (indicated by the solid arrow), focal adhesion sites were stained green by anti-vinculin and FITC-labeled secondary antibody (indicated by the dotted arrow), and cell nuclei were counterstained blue by Draq 5. Color images available online at www.liebertonline.com/tea

of *COL 1*, *HAS3*, *FSP-1*, *ALP*, and *AGG* (Fig. 1). When cells were cultured on the PGS-PCL scaffolds, the addition of CTGF significantly ($p < 0.05$) increased the mRNA levels of *HAS3* and *FSP-1*, while significantly ($p < 0.05$) suppressing the expression of *aP2* and *p53*. Compared to the conditioned TCPS culture, the introduction of CTGF to the PGS-PCL culture significantly ($p < 0.05$) attenuated the mRNA levels of *CD44*, *aP2*, and *ALP*, at the same time, dramatically elevated ($p < 0.01$) the expression of *FSP-1*. While CTGF led to 1.9 ± 0.3 -fold increase in the expression of *ALP* in the TCPS culture, it gave rise to a 0.9 ± 0.1 -fold decrease in the *ALP* expression in the PGS-PCL culture.

MSC preculture using PGS-PCL scaffolds without CTGF

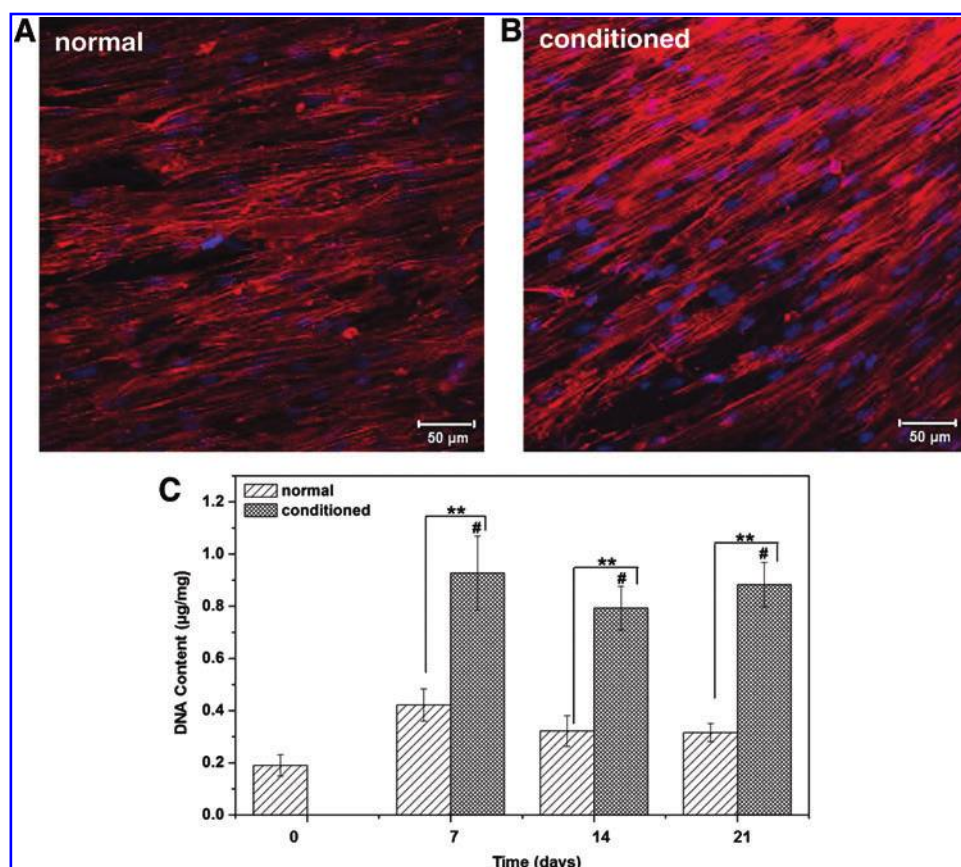
Electrospun PGS-PCL scaffolds were highly porous and exhibited consistent fiber morphology (Fig. 2A). The average fiber diameter was estimated to be $\sim 4 \mu\text{m}$ and the average mesh thickness was 100–150 μm. Fibers were randomly oriented and highly entangled. The PGS-PCL scaffolds were sparsely populated by the cells at the end of 3-day preculture. The majority of the cells retained by the scaffold

were stained green by the live/dead staining (Fig. 2B). Depth profiling of the confocal images revealed a homogeneous cell distribution 50 μm into the scaffold. Information regarding cell morphology and the degree of cell spreading was gleaned from the F-actin/vinculin costaining (Fig. 2C). The ability of the polymer fibers to absorb the nuclear dye (Draq 5) makes it possible to determine the relative location of the cells with respect to the individual fibers. MSCs readily attached to and elongated along the individual fibers, adopting a spread, spindle-shaped morphology. Early stress fibers (red stain, solid arrow) were visible along the edges of the cell body. Isolated, intense green spots, representative of focal adhesion complexes, could be detected at the cell termini along the long axis of the cell body (green stain, dotted arrow). Upon completion of the 3-day preculture, cells were incubated with or without CTGF for an additional 21 days.

Effects of CTGF on cell morphology and proliferation in PGS-PCL culture

The scaffold cellularity increased significantly during the first week of cultivation, in both normal (Fig. 3A) and conditioned culture (Fig. 3B). Cells adopted a spread-out

FIG. 3. Effects of CTGF on cell morphology (A, B) and scaffold cellularity (C). (A, B) MSCs were cultured in PGS-PCL scaffolds for 21 days in the normal (A) and conditioned (B) media and F-actin (red) and nuclei (blue) were stained by Alexa-568 phalloidin and DAPI, respectively. Images were obtained by merging confocal z-stack slices over 0–30 μ m sample depth. (C) Cell proliferation as assessed by picogreen DNA quantification. DNA content was normalized to the dry mesh weight. #Significant difference ($p < 0.05$) relative to the baseline level on day 0; **significant difference ($p < 0.05$) between normal and conditioned culture. Color images available online at www.liebertonline.com/tea



morphology with well-developed stress fibers transversing the entire cell body. Picogreen DNA assay was employed to obtain quantitative information on cell proliferation. Although the same number of cells was initially seeded, CTGF-conditioned scaffolds harbored more than twice as many cells as the control samples without CTGF on day 7 ($p < 0.05$, Fig. 3C). Prolonged culture in CTGF-containing media beyond day 7 did not lead to a significant change in DNA content per mg of dry constructs. Only a moderate increase in DNA content was observed in the control groups from day 0 to 7. The normalized DNA content in the CTGF-free control group was significantly ($p < 0.05$) lower than in the CTGF-treated samples at the respective time points.

Effects of CTGF on MSC differentiation in PGS-PCL culture

MSC differentiation was analyzed collectively by qPCR analyses and immunocytochemical and biochemical assays.

Quantitative PCR analysis. To gain fundamental understanding of the temporal effects of CTGF on MSCs cultivated on/in PGS-PCL scaffolds, the gene expression was normalized to the levels at day 0 (the end of day 3 pre-culture). *COL 1* gene expression (Fig. 4A) was significantly upregulated over the initial day 0 baseline level with or without CTGF, reaching a plateau at day 7. By day 21, cells expressed a significantly lower level of *COL 1* in the conditioned media (1.6 ± 0.1 -fold) than in the normal media (2.2 ± 0.1 -fold). Prolonged culture led to a significant ($p < 0.05$) upregulation of *ELA* gene expression relative to the

day 0 level (Fig. 4B) under all experimental conditions. The conditioned culture expressed similar level of *ELA* as the normal culture at all time points inspected. Cells residing in the PGS-PCL scaffolds consistently expressed a higher level of *DEC* in the conditioned media than in the corresponding normal media at days 7, 14, and 21 (Fig. 4C). Cells in the conditioned media expressed a significantly ($p < 0.05$) higher level of *DEC* (2.7 ± 0.3 -fold) than in the normal media (1.5 ± 0.2 -fold) at day 14. Similarly, *HAS3* (Fig. 4D) gene expression was drastically ($p < 0.05$) upregulated in the conditioned culture relative to the normal culture at day 7 and 14. The contribution of CTGF, however, was diminished at day 21. The *TIMP1* gene expression in the normal culture was significantly higher at day 21 than at day 0, and the addition of CTGF downregulated its expression back to the baseline level at day 0 (Fig. 4E). No statistically significant changes in *MMP1* gene expression were detected at various culture time with or without CTGF (data not shown).

Next, we examined the expression of essential markers for stem cell differentiation. The overall mRNA level of *CD44* (Fig. 5A) declined consistently throughout the study, and the addition of CTGF reinforced the decline. By day 21, *CD44* expression had decreased by $\sim 50\%$ relative to the baseline level in the conditioned culture. On the other hand, the mRNA level of *FSP-1* (Fig. 5B) was steadily and significantly upregulated in the presence of CTGF over the entire course of culture. In the absence of CTGF, only 2.3 ± 0.3 -fold increase relative to day 0 was observed in *FSP-1* expression, whereas over 40 ± 13 -fold increase in *FSP-1* expression was detected at day 21 in the conditioned culture. The potential of MSCs to undergo classical tri-lineage differentiation was also analyzed.

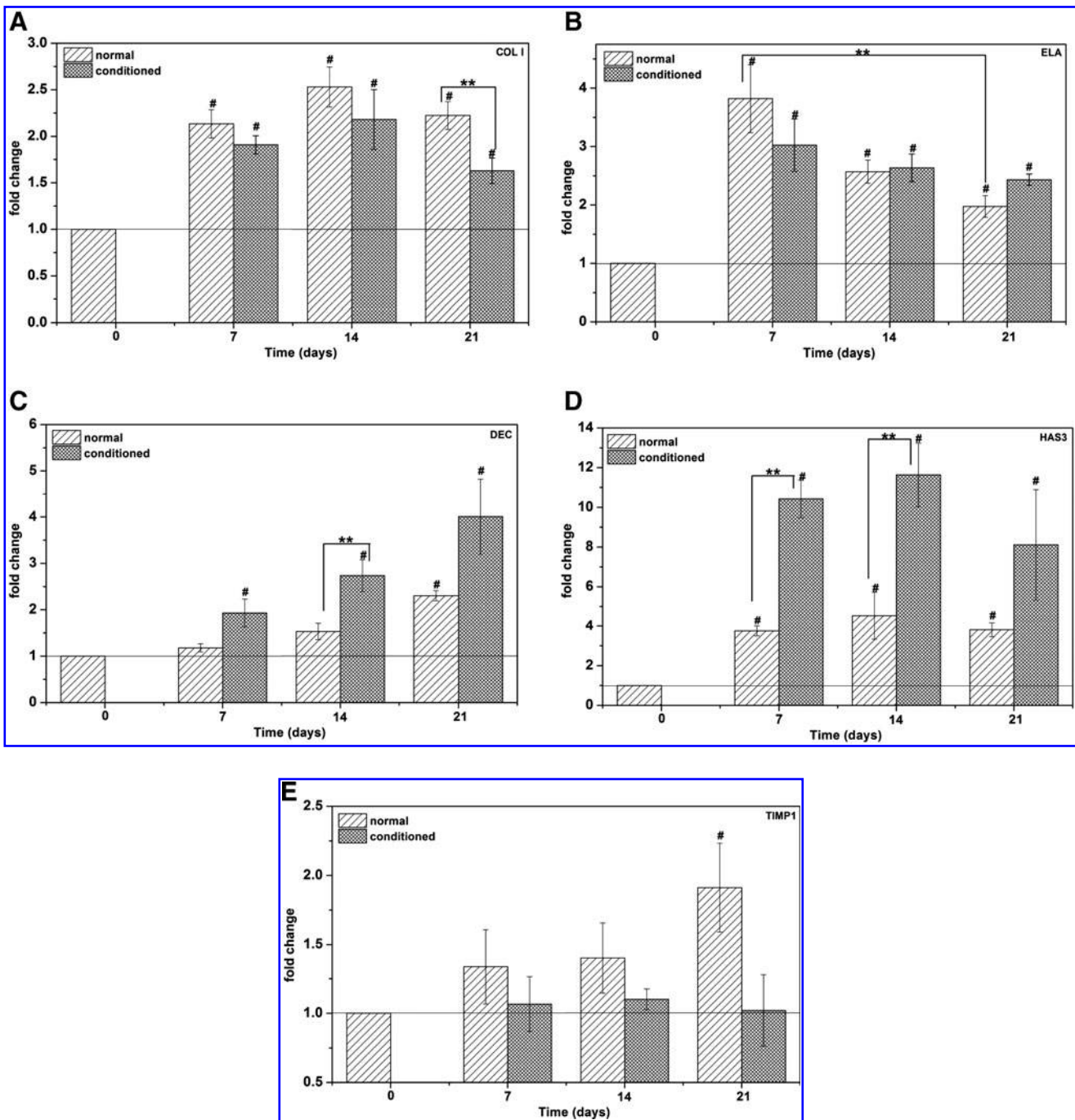


FIG. 4. Effects of CTGF supplement on the gene expression of MSCs cultured on/in PGS-PCL scaffolds. **(A)** COL I; **(B)** ELA; **(C)** DEC; **(D)** HAS3; and **(E)** TIMP1. GAPDH was used as internal control and the relative gene expression was normalized to the baseline level at day 0 as indicated by the solid line. [#]Significant difference ($p < 0.05$) relative to the baseline level at day 0; ^{**}significant difference ($p < 0.05$) between the normal and the conditioned culture **(A, C, E)** or between day 7 and 21 normal culture **(B)**. COL I, collagen type I; ELA, elastin; DEC, decorin; TIMP1, tissue inhibitor of metalloproteinases 1; HAS3, HA synthase 3.

The mRNA levels of AGG (Fig. 5C), ALP (Fig. 5D) and *aP2* (Fig. 5E) were used as the indicator of chondrogenesis, osteogenesis, and adipogenesis, respectively. The mRNA level of AGG was significantly upregulated relative to day 0 in the conditioned culture at day 7 and 21 ($p < 0.05$). Cells expressed higher level of ALP at day 7 and 21, relative to day 0 in the normal media. The addition of CTGF attenuated this trend, most significantly ($p < 0.05$) at day 21 when the ALP expres-

sion dropped below the baseline level for the conditioned culture. With the exception of day 21 for the normal culture, a significant decrease in *aP2* expression relative to day 0 was observed at day 7 and 14, in both normal and conditioned cultures. By day 21, the PGS-PCL/CTGF culture exhibited a 95% decrease in *aP2* expression, in sharp contrast to the elevated level (1.4 ± 0.4 -fold) detected from PGS-PCL culture in normal medium. Finally, the pro-apoptotic factor *p53* mRNA

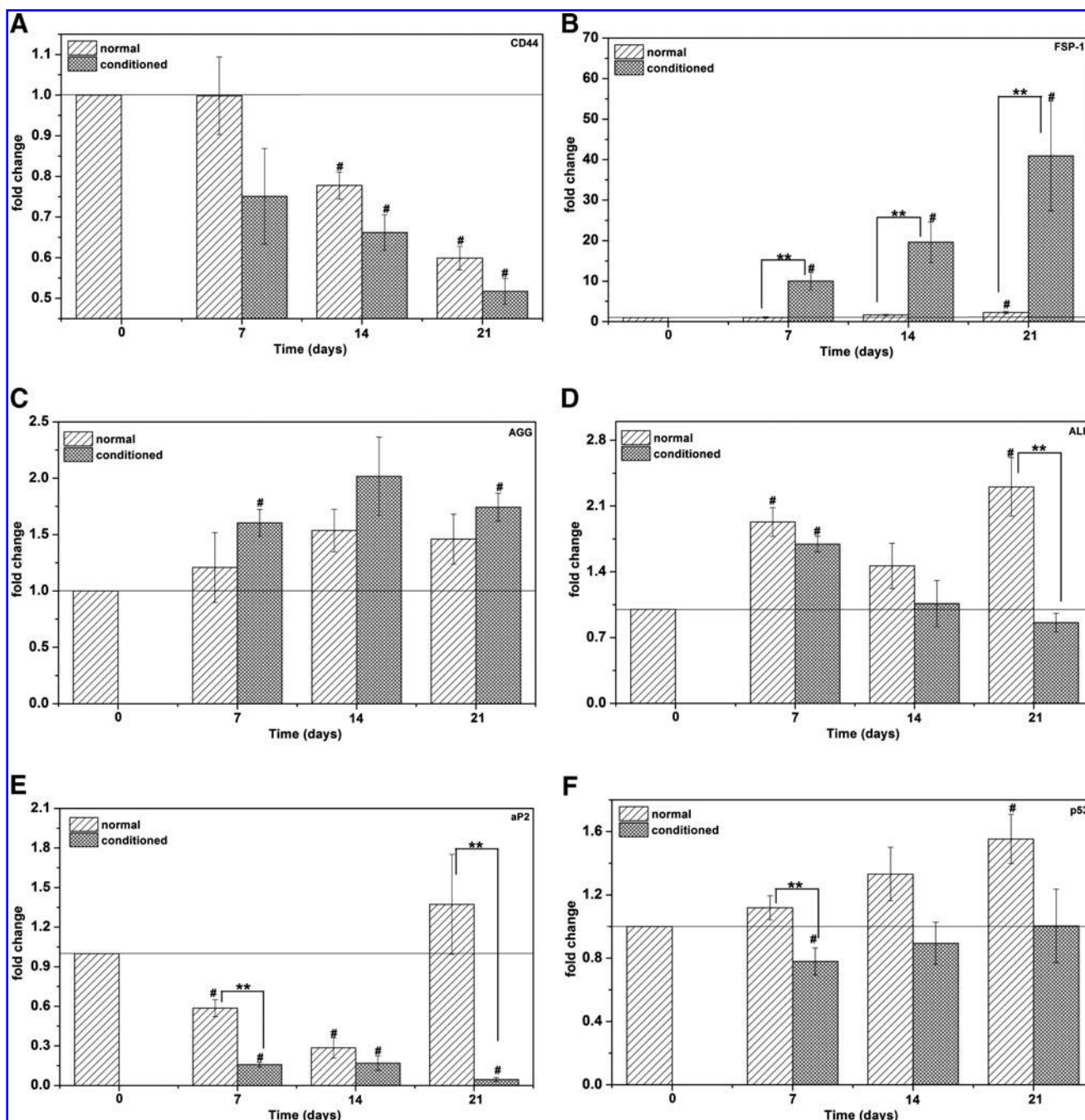


FIG. 5. Effects of CTGF supplement on the gene expression of MSCs cultured on/in PGS-PCL scaffolds. **(A)** *CD44*; **(B)** *FSP-1*; **(C)** *AGG*; **(D)** *ALP*; **(E)** *aP2*; and **(F)** *p53*. *GAPDH* was used as internal control and the relative gene expression was normalized to the baseline level at day 0 as indicated by the solid line. #Significant difference ($p < 0.05$) relative to the baseline level at day 0; **significant difference ($p < 0.05$) between the normal and the conditioned culture. *FSP-1*, fibroblast-specific protein-1; *ALP*, alkaline phosphatase; *AGG*, aggrecan.

level was examined (Fig. 5F). The normal media consistently induced a higher *p53* expression than the conditioned media at day 7. While cells expressed a higher level of *p53* when cultured in the normal media at day 21, their expression was close to the baseline level if CTGF was introduced.

Immunocytochemical and biochemical analysis. MSC differentiation was analyzed semi-quantitatively at the protein level using standard immunocytochemical assays.

Stronger STRO-1 staining was detected from PGS-PCL cultures than from PGS-PCL/CTGF cultures (Fig. 6A, B). Cells residing in PGS-PCL scaffolds were stained negative for MSA (Fig. 6C, D), irrespective of the medium composition. Immunocytochemical analyses for COL I and III were performed at various times, and representative confocal images were shown in Supplementary Figures S1 and S2, respectively (Supplementary Data are available online at www.liebertonline.com/tea). At day 0, the fluorescence

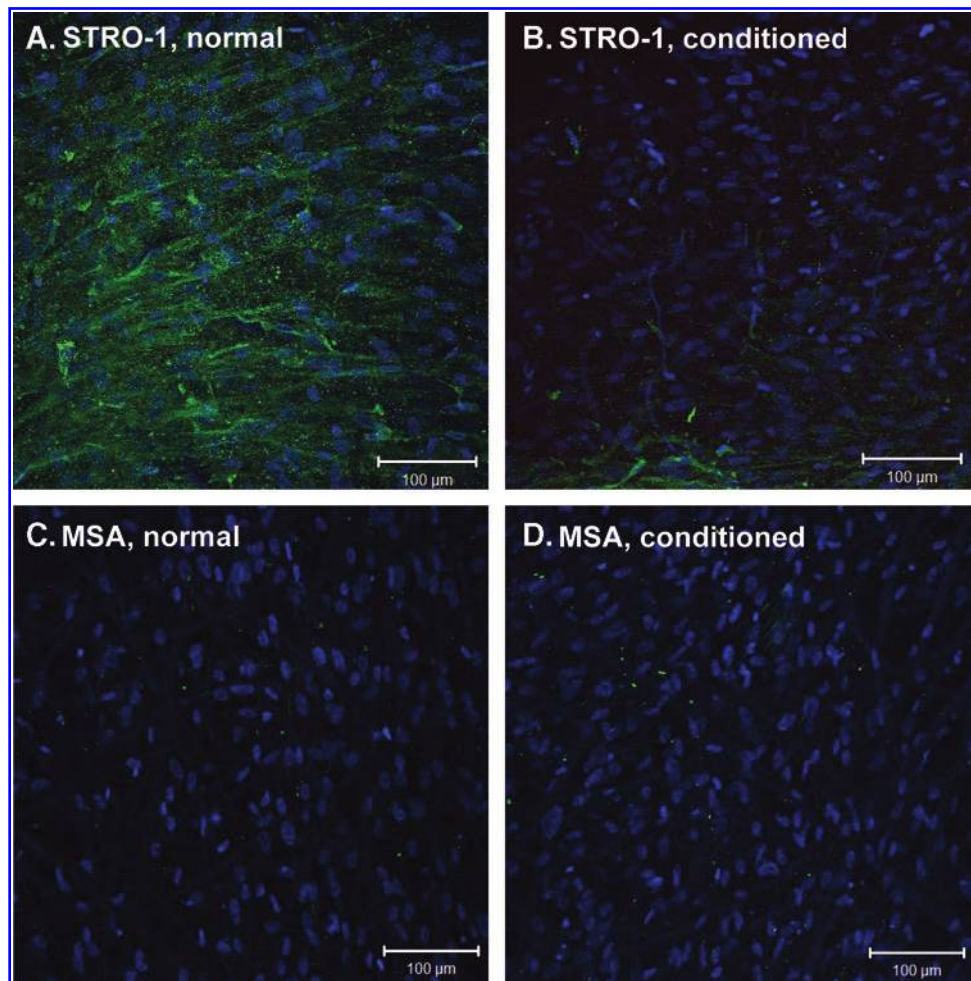


FIG. 6. Immunocytochemical staining for STRO-1 and MSA. (A, B) STRO-1 staining of PGS-PCL cultures in normal (A) and conditioned media (B) at day 14; (C, D) MSA staining of PGS-PCL cultures in the normal (C) and the conditioned (D) media at day 21. MSA, muscle-specific actin. Color images available online at www.liebertonline.com/tea

intensity for COL I and III was low. Interestingly, while COL I clustered around the cells in the normal culture at day 14 and 21, it was abundantly distributed in the extracellular space in the conditioned media. Total COL I production increased dramatically during the first week of conditioned culture (Fig. 7A); thereafter, the COL I content remained unchanged. Average COL I content in normal PGS-PCL culture increased moderately during the 3 weeks of culture. The conditioned culture showed a significantly ($p < 0.05$) higher amount of COL I than the normal medium at all times. A similar trend was observed for COL III (Fig. 7B).

Additional biochemical analyses were performed to quantify the ability of cells to synthesize sGAG and ELA under various conditions. Figure 8A reveals that the addition of CTGF in the culture media resulted in a steady increase in sGAG production over the entire course of culture. The sGAG production was significantly ($p < 0.05$) higher in the conditioned culture than in the normal culture. By day 21, CTGF-treated constructs contained an average $4.9 \pm 0.3 \mu\text{g}$ sGAG per mg dry constructs, whereas cells in the normal media only produced $0.9 \pm 0.3 \mu\text{g}$ sGAG per mg dry constructs. Overall, the addition of CTGF led to over fivefold increase ($p < 0.05$) in sGAG production. Similarly, the addi-

tion of CTGF gave rise to an increase in ELA production. Average ELA deposition (Fig. 8B) in the conditioned groups was remarkably ($p < 0.001$) elevated at day 7 and 14, relative to day 0. ELA content was significantly higher ($p < 0.05$) in the conditioned groups than in the normal controls at day 7 and 14. An estimated 33.7 ± 2.5 and $16.3 \pm 2.0 \mu\text{g}$ ELA was produced per mg construct at day 7 in the conditioned culture and normal culture, respectively.

Discussion

The multi-potent nature of bone marrow-derived MSCs³⁷ and the putative mesenchymal origin of fibroblasts^{29,38} motivated us to explore the fibroblastic differentiation potential of MSCs for vocal fold regeneration. In this study, polyester-based PGS-PCL scaffolds were employed to provide a cell-support stem cell niche. We showed that the fibroblastic differentiation of MSCs can be modulated by a synthetic, fibrous scaffold supplemented with CTGF. CTGF regulates cell adhesion, migration, proliferation, gene expression, differentiation, and survival primarily through direct binding to specific integrin receptors and heparan sulfate proteoglycans.³⁹ The ability of CTGF to significantly upregulate the

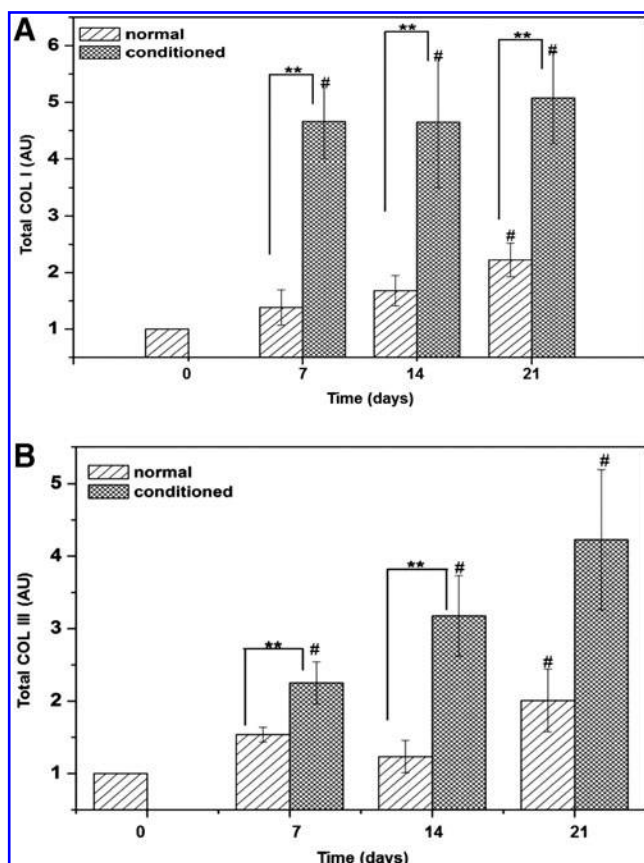


FIG. 7. Semi-quantitative analysis of total COL I (A) and COL III (B) deposition by MSCs in PGS-PCL scaffolds cultured in normal and conditioned media. #Significant difference ($p < 0.05$) relative to the baseline level at day 0; **significant difference ($p < 0.05$) between normal and conditioned constructs.

gene expression of *FSP-1* and downregulate the expression of *CD44*, *aP2*, and *ALP* by cells cultured in PGS-PCL scaffolds (Fig. 1) as compared to those plated on traditional TCPS substrates suggests that the fibrous scaffold is more conducive to the fibroblastic differentiation, and less supportive of the classical tri-lineage differentiation. The 3D fibrous scaffolds provide a more biomimetic microenvironment that may potentiate the effects of CTGF on the fibroblastic differentiation of MSCs. In theory, the differentiated cells can continue to produce tissue-specific ECM *in situ* under physiologically relevant conditions and the cellular constructs can be easily manipulated for implantation purposes.

A 3-day preculture in MSC maintenance media was necessary for the establishment of cell-matrix connection and a baseline for the subsequent time-course studies. The PGS-PCL scaffolds supported the attachment of MSCs; cells spread along the microfibers through the focal adhesion complexes, and adopted a typical fibroblast-like morphology 3 days postseeding (Fig. 2C). The inter-fiber space was suitable for cell migration and infiltration. The ability of MSCs to remodel the newly deposited matrix may further facilitate the cell infiltration into the bulk of the scaffolds.⁴⁰ The adherent MSCs continued to assume the same morphology during the subsequent conditioned culture (Fig. 3A, B). MSCs can be readily expanded during the first week of culture in the conditioned

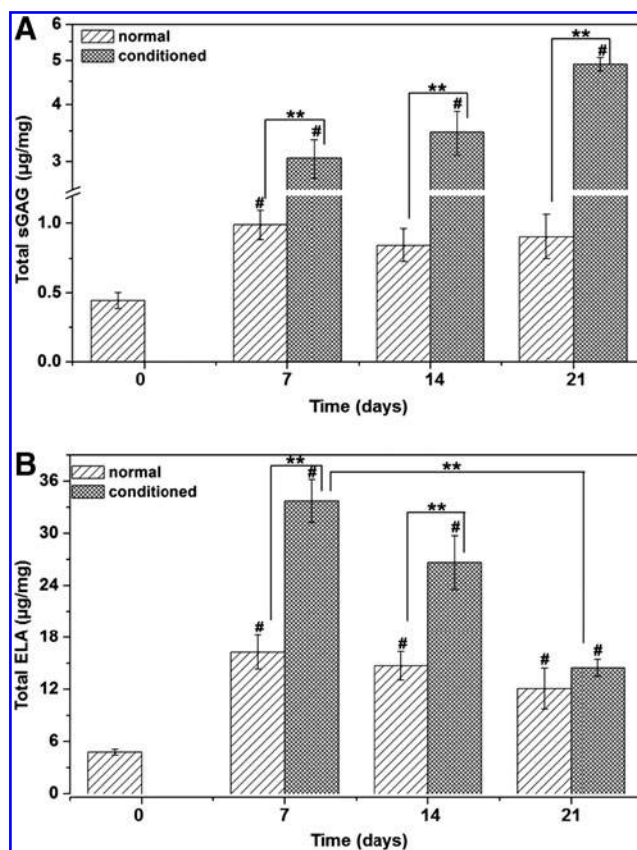


FIG. 8. Biochemical quantification of total sGAG (A) and ELA (B) synthesis by MSCs in PGS-PCL scaffolds cultured in normal and conditioned media. #Significant difference ($p < 0.05$) relative to the baseline level at day 0; **significant difference ($p < 0.05$) between normal and conditioned constructs or between day 7 and 21 conditioned culture. sGAG, sulfated glycosaminoglycan.

media. The higher proliferation rate (Fig. 3C) observed in the conditioned culture can be attributed to CTGF's role in promoting cell proliferation.²⁸ After reaching confluence at day 7, cell division was halted. The lack of cell proliferation after day 7 implies potential engagement in differentiation.⁴¹

The commitment of MSCs to the fibroblast phenotype is evidenced collectively by the attenuation of multi-potent mesenchymal markers *CD44* (Fig. 5A)⁴² and *STRO-1* (Fig. 6A, B),⁴³ and simultaneous enhancement in the expression of *FSP-1*, a fibroblast markers that was originally identified in epithelial-mesenchymal transition.³⁰ qPCR analyses of *ALP* and *aP2* further confirmed that the osteogenesis and adipogenesis potentials of MSCs are significantly suppressed in our culture system in the presence of CTGF (Fig. 5D, E). The inability of CTGF to suppress AGG expression (Fig. 5C) can be attributed to CTGF's role in chondrogenesis⁴⁴ and high cell density in the PGS-PCL/CTGF constructs. The differentiation of MSCs to myofibroblasts is ruled out by the negative MSA staining (Fig. 6C, D).⁴⁵ This finding demonstrates that CTGF-stimulated fibroblastic differentiation process is distinctly different from fibrosis, which is characterized by the major myofibroblastic commitment and MSA-positive cell population.²⁹

COL I and III are two major collagenous fibers contributing to the tensile strength of connective tissue ECM.⁴⁶ They

have also been employed as broad molecular marker for fibroblastic differentiation.^{29,47} Another fibrous protein, ELA, is critical for maintaining tissue elasticity.⁴⁸ The mRNA level of *COL I* in the conditioned PGS-PCL culture was lower than that in the normal media at day 21 (Fig. 4A). Contrarily, our protein level analysis also showed an elevated amount COL I and III accumulation upon addition of CTGF (Fig. 7). The mRNA level of *ELA* was not significantly influenced by CTGF (Fig. 4B). However, the addition of CTGF to PGS-PCL cultures led to an increase in ELA synthesis at day 7 and 14 (Fig. 8B). It should be emphasized that gene regulation and protein synthesis are two separate, time-dependent events.^{46,49} Previous studies have shown that CTGF can regulate the production of ECM proteins without affecting their mRNA levels, implying that the regulation may occur during post-translational events of protein biosynthesis.^{50,51} CTGF may have enhanced the production or activity of proteins or enzymes involved in protein modification or assembly rather than the peptide precursors themselves.⁵² The significant and consistent enhancement of *DEC* gene expression by exogenous CTGF confirms our speculation because of DEC's role in assisting collagen fibril assembly.^{53,54} In the case of ELA, the activity of ELA post-translational enzymes (for example, lysal oxidase) may have been activated by CTGF in our particular culture system.⁵²

In addition to structural proteins, amorphous GAG molecules in connective tissues establish a highly hydrated network facilitating the rapid diffusion of nutrients, metabolites, and hormones.⁴⁶ Many GAG molecules also contribute to the maintenance of proper tissue viscoelasticity.^{53,55} The upregulation of *HAS3* gene expression (Fig. 4D) by exogenous CTGF suggests the improved ability of cells to synthesize HA. The significant enhancement in cellular sGAG deposition upon CTGF addition may be attributed to the ability of the newly synthesized sGAG to sequester the exogenous CTGF, thereby potentiating its biological functions.^{39,56} The homeostasis of the connective tissue is maintained by the resident fibroblasts through the synthesis and degradation of ECM components. While MMP1 breaks down the interstitial collagens, TIMP1 generally inhibits against a wide range of MMPs, including MMP1.⁵⁷ Our results show that expression of both *MMP1* and *TIMP1* is insensitive to CTGF supplement. Therefore, MSCs cultivated on/in the fibrous scaffolds may not be actively involved in ECM remodeling.

This study represents our initial effort in assessing the applicability of fibrous PGS-PCL scaffolds, combined with an exogenous regulatory factor, to foster the adhesion, proliferation, and fibroblastic differentiation of MSCs. In our study, cells residing in the scaffolds were cultivated in CTGF-supplemented media under static conditions. For successful differentiation of MSCs to vocal fold-like fibroblasts, physiologically relevant vibration stimulations may need to be imposed on the cultured MSCs⁵⁸ because the dynamic motion of the vocal folds not only is indispensable for producing high quality sound but also contributes, at least in part, to the development and maturation of vocal folds.⁵⁹ For the successful assembly of functional tissues *in vitro*, the regulatory factor must be presented to the cells in a controlled manner with a desired spatio/temporal pattern. We are currently conducting systematic investigations assessing MSC differentiation and the matrix remodeling. Results obtained from these studies will be reported in due course.

Conclusion

Polyester-based fibrous scaffolds and soluble CTGF were employed to create a conducive microenvironment for the fibroblastic differentiation of MSCs. The PGS-PCL scaffolds supported the attachment and the proliferation of MSCs. Cells infiltrated readily into the bulk of the scaffolds, adopting a spindle-shaped morphology without undergoing myogenesis. The addition of CTGF significantly enhanced cell proliferation, decreased the expression of stem cell markers, and increased the expression of fibroblastic hallmarks. Cells residing in the fibrous scaffolds were more susceptible to CTGF-mediated fibroblast differentiation than those grown on traditional TCPS plates. The presence of CTGF contributed to the altered productivity of essential ECM proteins, including COL I/III, ELA, HAS3, DEC, and sGAG. The differentiated MSCs exhibited a diminished potential to become osteoblasts, chondrocytes, and adipocytes. Our future efforts are directed toward the creation of a vocal fold-like stem cell niche using fibrous scaffolds combined with spatio/temporal presentation of CTGF and dynamic mechanical environments similar to the vocal fold-like vibrations.

Acknowledgments

We thank Alexandra Farran and Fang Jia for their technical assistance and Dr. Jeremy Mao for the stimulating discussions. We also thank Drs. Kirk Czymmek and Jeffrey Caplan for their training and advice on confocal imaging. This work is funded by National Institutes of Health (NIDCD, R01 008965 to X.J.) and University of Delaware Faculty Startup Funds (to X.J.). A.K. acknowledges funding from the National Institutes of Health (EB009196, DE019024, EB007249, HL099073, and AR057837), the National Science Foundation CAREER Award (DMR 0847287), and the Office of Naval Research Young Investigator Award. S.S. is grateful for the postdoctoral fellowship awarded by Fonds de Recherche sur la Nature et les Technologies (FQRNT), Quebec, Canada.

Disclosure Statement

No competing financial interests exist.

References

- Gray, S.D. Cellular physiology of the vocal folds. *Otolaryngol Clin North Am* **33**, 679, 2000.
- Titze, I.R. *Principles of Voice Production*. NJ: Prentice-Hall, 1994.
- Hirano, S. Current treatment of vocal fold scarring. *Curr Opin Otolaryngol Head Neck Surg* **13**, 143, 2005.
- Chen, X., and Thibeault, S.L. Novel isolation and biochemical characterization of immortalized fibroblasts for tissue engineering vocal fold lamina propria. *Tissue Eng Part C Methods* **15**, 201, 2009.
- Parekkadan, B., and Milwid, J.M. Mesenchymal stem cells as therapeutics. *Annu Rev Biomed Eng* **12**, 87, 2010.
- Pittenger, M.F., Mackay, A.M., Beck, S.C., Jaiswal, R.K., Douglas, R., Mosca, J.D., *et al.* Multilineage potential of adult human mesenchymal stem cells. *Science* **284**, 143, 1999.
- Bae, S., Ahn, J.H., Park, C.W., Son, H.K., Kim, K.S., Lim, N.K., *et al.* Gene and microRNA expression signatures of

- human mesenchymal stromal cells in comparison to fibroblasts. *Cell Tissue Res* **335**, 565, 2009.
8. Halfon, S., Abramov, N., Grinblat, B., and Ginis, I. Markers distinguishing mesenchymal stem cells from fibroblasts are downregulated with passaging. *Stem Cells Dev* **20**, 53, 2011.
 9. Ishii, M., Koike, C., Igarashi, A., Yamanaka, K., Pan, H., Higashi, Y., *et al.* Molecular markers distinguish bone marrow mesenchymal stem cells from fibroblasts. *Biochem Biophys Res Commun* **332**, 297, 2005.
 10. Grayson, W.L., Zhao, F., Izadpanah, R., Bunnell, B., and Ma, T. Effects of hypoxia on human mesenchymal stem cell expansion and plasticity in 3d constructs. *J Cell Physiol* **207**, 331, 2006.
 11. Junker, J.P., Sommar, P., Skog, M., Johnson, H., and Kratz, G. Adipogenic, chondrogenic and osteogenic differentiation of clonally derived human dermal fibroblasts. *Cells Tissues Organs* **191**, 105, 2010.
 12. Kurpinski, K., Chu, J., Hashi, C., and Li, S. Anisotropic mechanosensing by mesenchymal stem cells. *Proc Natl Acad Sci USA* **103**, 16095, 2006.
 13. Lim, S.H., and Mao, H.Q. Electrospun scaffolds for stem cell engineering. *Adv Drug Deliv Rev* **61**, 1084, 2009.
 14. Place, E.S., Evans, N.D., and Stevens, M.M. Complexity in biomaterials for tissue engineering. *Nat Mater* **8**, 457, 2009.
 15. Reneker, D.H., and Chun, I. Nanometre diameter fibres of polymer, produced by electrospinning. *Nanotechnology* **7**, 216, 1996.
 16. Mauck, R.L., Baker, B.M., Nerurkar, N.L., Burdick, J.A., Li, W.J., Tuan, R.S., *et al.* Engineering on the straight and narrow: the mechanics of nanofibrous assemblies for fiber-reinforced tissue regeneration. *Tissue Eng Part B Rev* **15**, 171, 2009.
 17. Goldberg, M., Langer, R., and Jia, X.Q. Nanostructured materials for applications in drug delivery and tissue engineering. *J Biomater Sci Polym Ed* **18**, 241, 2007.
 18. Khademhosseini, A., Vacanti, J.P., and Langer, R. Progress in tissue engineering. *Sci Am* **300**, 64, 2009.
 19. Sant, S., Hwang, C.M., Lee, S.H., and Khademhosseini, A. Hybrid PGS-PCL microfibrillar scaffolds with improved mechanical and biological properties. *J Tissue Eng Regen Med* **5**, 283, 2011.
 20. Yi, F., and LaVan, D.A. Poly(glycerol sebacate) nanofiber scaffolds by core/shell electrospinning. *Macromol Biosci* **8**, 803, 2008.
 21. Chen, Q.Z., Bismarck, A., Hansen, U., Junaid, S., Tran, M.Q., Harding, S.E., *et al.* Characterisation of a soft elastomer poly(glycerol sebacate) designed to match the mechanical properties of myocardial tissue. *Biomaterials* **29**, 47, 2008.
 22. Radisic, M., Park, H., Martens, T.P., Salazar-Lazaro, J.E., Geng, W., Wang, Y., *et al.* Pre-treatment of synthetic elastomeric scaffolds by cardiac fibroblasts improves engineered heart tissue. *J Biomed Mater Res A* **86**, 713, 2008.
 23. Redenti, S., Neeley, W.L., Rompani, S., Saigal, S., Yang, J., Klassen, H., *et al.* Engineering retinal progenitor cell and scrollable poly(glycerol-sebacate) composites for expansion and subretinal transplantation. *Biomaterials* **30**, 3405, 2009.
 24. Wang, Y., Ameer, G.A., Sheppard, B.J., and Langer, R. A tough biodegradable elastomer. *Nat Biotechnol* **20**, 602, 2002.
 25. Ifkovits, J.L., Devlin, J.J., Eng, G., Martens, T.P., Vunjak-Novakovic, G., and Burdick, J.A. Biodegradable fibrous scaffolds with tunable properties formed from photo-cross-linkable poly(glycerol sebacate). *ACS Appl Mater Interfaces* **1**, 1878, 2009.
 26. Brigstock, D.R. The connective tissue growth factor cysteine-rich 61 nephroblastoma overexpressed (ccn) family. *Endocr Rev* **20**, 189, 1999.
 27. Moussad, E., and Brigstock, D.R. Connective tissue growth factor: What's in a name? *Mol Genet Metab* **71**, 276, 2000.
 28. Perbal, B. Ccn proteins: Multifunctional signalling regulators. *Lancet* **363**, 62, 2004.
 29. Lee, C.H., Shah, B., Moioli, E.K., and Mao, J.J. Ctgf directs fibroblast differentiation from human mesenchymal stem/stromal cells and defines connective tissue healing in a rodent injury model. *J Clin Invest* **120**, 3340, 2010.
 30. Strutz, F., Okada, H., Lo, C.W., Danoff, T., Carone, R.L., Tomaszewski, J.E., *et al.* Identification and characterization of a fibroblast marker: Fsp1. *J Cell Biol* **130**, 393, 1995.
 31. Wise, J.K., Yarin, A.L., Megaridis, C.M., and Cho, M. Chondrogenic differentiation of human mesenchymal stem cells on oriented nanofibrous scaffolds: Engineering the superficial zone of articular cartilage. *Tissue Eng Part A* **15**, 913, 2009.
 32. Farran, A.J.E., Teller, S.S., Jha, A.K., Jiao, T., Hule, R.A., Clifton, R.J., *et al.* Effects of matrix composition, microstructure, and viscoelasticity on the behaviors of vocal fold fibroblasts cultured in three-dimensional hydrogel networks. *Tissue Eng Part A* **16**, 1247, 2010.
 33. Chomczynski, P., and Sacchi, N. Single-step method of rna isolation by acid guanidinium thiocyanate-phenol-chloroform extraction. *Anal Biochem* **162**, 156, 1987.
 34. Chomczynski, P. A reagent for the single-step simultaneous isolation of RNA, DNA and proteins from cell and tissue samples. *Biotechniques* **15**, 532, 1993.
 35. Pfaffl, M.W. A new mathematical model for relative quantification in real-time rt-pcr. *Nucleic Acids Res* **29**, e45, 2001.
 36. Tanaka, H., Murphy, C.L., Murphy, C., Kimura, M., Kawai, S., and Polak, J.M. Chondrogenic differentiation of murine embryonic stem cells: effects of culture conditions and dexamethasone. *J Cell Biochem* **93**, 454, 2004.
 37. Caplan, A.I. Adult mesenchymal stem cells for tissue engineering versus regenerative medicine. *J Cell Physiol* **213**, 341, 2007.
 38. Eyden, B. The myofibroblast: a study of normal, reactive and neoplastic tissues, with an emphasis on ultrastructure. Part 1—normal and reactive cells. *J Submicrosc Cytol Pathol* **37**, 109, 2005.
 39. Chen, C.C., and Lau, L.F. Functions and mechanisms of action of ccn matricellular proteins. *Int J Biochem Cell Biol* **41**, 771, 2009.
 40. Daley, W.P., Peters, S.B., and Larsen, M. Extracellular matrix dynamics in development and regenerative medicine. *J Cell Sci* **121**, 255, 2008.
 41. Itahana, K., Dimri, G.P., Hara, E., Itahana, Y., Zou, Y., Desprez, P.Y., *et al.* A role for p53 in maintaining and establishing the quiescence growth arrest in human cells. *J Biol Chem* **277**, 18206, 2002.
 42. Park, E., and Patel, A.N. Changes in the expression pattern of mesenchymal and pluripotent markers in human adipose-derived stem cells. *Cell Biol Int* **34**, 979, 2010.
 43. Simmons, P.J., and Torokstorb, B. Identification of stromal cell precursors in human bone-marrow by a novel monoclonal-antibody, stro-1. *Blood* **78**, 55, 1991.
 44. Nakanishi, T., Nishida, T., Shimo, T., Kobayashi, K., Kubo, T., Tamatani, T., *et al.* Effects of ctgf/hcs24, a product of a hypertrophic chondrocyte-specific gene, on the proliferation and differentiation of chondrocytes in culture. *Endocrinology* **141**, 264, 2000.

45. Tsukada, T., Tipples, D., Gordon, D., Ross, R., and Gown, A.M. Hh35, a muscle-actin-specific monoclonal antibody. I. Immunocytochemical and biochemical characterization. *Am J Pathol* **126**, 51, 1987.
46. Alberts, B., Johnson, A., Lewis, J., Raff, M., Roberts, K., and Walter, P. *Molecular Biology of the Cell*, 4th edition. NY: Garland Science, 2002.
47. Altman, G.H., Horan, R.L., Martin, I., Farhadi, J., Stark, P.R., Volloch, V., *et al.* Cell differentiation by mechanical stress. *FASEB J* **16**, 270, 2002.
48. Perlman, A.L., Titze, I.R., and Cooper, D.S. Elasticity of canine vocal fold tissue. *J Speech Hear Res* **27**, 212, 1984.
49. Prockop, D.J., and Kivirikko, K.I. Collagens—molecular biology, diseases, and potentials for therapy. *Annu Rev Biochem* **64**, 403, 1995.
50. Heng, E.C., Huang, Y., Black, S.A., Jr., and Trackman, P.C. Ccn2, connective tissue growth factor, stimulates collagen deposition by gingival fibroblasts via α 3 and α 6- and β 1 integrins. *J Cell Biochem* **98**, 409, 2006.
51. Hong, H.H., Uzel, M.I., Duan, C., Sheff, M.C., and Trackman, P.C. Regulation of lysyl oxidase, collagen, and connective tissue growth factor by $\text{tgf-}\beta$ 1 and detection in human gingiva. *Lab Invest* **79**, 1655, 1999.
52. Oleggini, R., Gastaldo, N., and Di Donato, A. Regulation of elastin promoter by lysyl oxidase and growth factors: cross control of lysyl oxidase on TGF- β 1 effects. *Matrix Biol* **26**, 494, 2007.
53. Hahn, M.S., Jao, C.Y., Faquin, W., and Grande-Allen, K.J. Glycosaminoglycan composition of the vocal fold lamina propria in relation to function. *Ann Otol Rhinol Laryngol* **117**, 371, 2008.
54. Iwasaki, S., Hosaka, Y., Iwasaki, T., Yamamoto, K., Nagayasu, A., Ueda, H., *et al.* The modulation of collagen fibril assembly and its structure by decorin: an electron microscopic study. *Arch Histol Cytol* **71**, 37, 2008.
55. Lujan, T.J., Underwood, C.J., Jacobs, N.T., and Weiss, J.A. Contribution of glycosaminoglycans to viscoelastic tensile behavior of human ligament. *J Appl Physiol* **106**, 423, 2009.
56. Farach-Carson, M.C., Hecht, J.T., and Carson, D.D. Heparan sulfate proteoglycans: key players in cartilage biology. *Crit Rev Eukaryot Gene Expr* **15**, 29, 2005.
57. Woessner, J.F. Mmps and tims—an historical perspective. *Mol Biotechnol* **22**, 33, 2002.
58. Jia, X., Jia, M., Jha, A.K., Farran, A.J.E., and Tong, Z. Dynamic vibrational method and device for vocal fold tissue growth. 2010.
59. Hartnick, C.J., Rehbar, R., and Prasad, V. Development and maturation of the pediatric human vocal fold lamina propria. *Laryngoscope* **115**, 4, 2005.
60. Seo, J.Y., Lee, S.H., Youn, C.S., Choi, H.R., Rhie, G.E., Cho, K.H., *et al.* Ultraviolet radiation increases tropoelastin mRNA expression in the epidermis of human skin *in vivo*. *J Invest Dermatol* **116**, 915, 2001.
61. Chen, C.H., Tsai, J.L., Wang, Y.H., Lee, C.L., Chen, J.K., and Huang, M.H. Low-level laser irradiation promotes cell proliferation and mRNA expression of type I collagen and decorin in porcine Achilles tendon fibroblasts *in vitro*. *J Orthop Res* **27**, 646, 2009.
62. Chen, X., and Thibeault, S.L. Biocompatibility of a synthetic extracellular matrix on immortalized vocal fold fibroblasts in 3-d culture. *Acta Biomater* **6**, 2940, 2010.
63. Ruster, B., Gottig, S., Ludwig, R.J., Bistran, R., Muller, S., Seifried, E., *et al.* Mesenchymal stem cells display coordinated rolling and adhesion behavior on endothelial cells. *Blood* **108**, 3938, 2006.
64. Imaizumi, T., Arikawa, T., Sato, T., Uesato, R., Matsumiya, T., Yoshida, H., *et al.* Involvement of retinoic acid-inducible gene-1 in inflammation of rheumatoid fibroblast-like synoviocytes. *Clin Exp Immunol* **153**, 240, 2008.
65. Astori, G., Vignati, F., Bardelli, S., Tubio, M., Gola, M., Albertini, V., *et al.* "In vitro" and multicolor phenotypic characterization of cell subpopulations identified in fresh human adipose tissue stromal vascular fraction and in the derived mesenchymal stem cells. *J Transl Med* **5**, 55, 2007.
66. Chung, C., and Burdick, J.A. Influence of three-dimensional hyaluronic acid microenvironments on mesenchymal stem cell chondrogenesis. *Tissue Eng Part A* **15**, 243, 2009.
67. Wuertz, K., Godburn, K., and Iatridis, J.C. Msc response to pH levels found in degenerating intervertebral discs. *Biochem Biophys Res Commun* **379**, 824, 2009.
68. Ryan, D.H., Nuccie, B.L., Ritterman, I., Liesveld, J.L., Abboud, C.N., and Insel, R.A. Expression of interleukin-7 receptor by lineage-negative human bone marrow progenitors with enhanced lymphoid proliferative potential and b-lineage differentiation capacity. *Blood* **89**, 929, 1997.

Address correspondence to:

Xinqiao Jia, Ph.D.

Department of Materials Science and Engineering

Delaware Biotechnology Institute

University of Delaware

Newark, DE 19716

E-mail: xjia@udel.edu

Ali Khademhosseini, Ph.D.

Department of Medicine

Center for Biomedical Engineering

Brigham and Women's Hospital

Harvard Medical School

Cambridge, MA 02139

E-mail: alik@rics.bwh.harvard.edu

Received: April 16, 2011

Accepted: June 17, 2011

Online Publication Date: July 29, 2011

